J Mater Sci (2007) 42:4996–5002
DOI 10.1007/s10853-006-0610-x

Synthesis of tunable sized capped magnetic iron oxide nanoparticles highly soluble in organic solvents

Panagiotis Dallas · Athanasios B. Bourlinos · Dimitrios Niarchos · Dimitrios Petridis

Received: 16 May 2006 / Accepted: 21 June 2006 / Published online: 23 February 2007

Abstract Surface modification of magnetic nanoparticles by organic surfactants is known to provide them with solubility in organic solvents (ferrofluids), which undoubtedly is an important property in several applications and studies. In this report, the main interest is focused on structural, magnetic and adsorption properties of iron oxide nanoparticles that are derived under water/toluene biphase conditions in the presence of oleic acid or oleylamine as the capping agents. The surfactants provide them with excellent stability and solubility in organic solvents like toluene or chloroform. Furthermore, by adding the appropriate surfactant or altering the temperature of the aqueous phase at the initial stage of the reaction we achieve a size control of the nanoparticles within the range 6–18 nm. The presence of capping agents or high reaction temperatures favours the formation of smaller nanoparticles. The adsorption of the surfactants (chemisorption) was identified with FT-IR spectroscopy, while Mössbauer studies have been performed to representative samples in order to identify the presence of either γ-Fe_2O_3 or Fe_3O_4, depending on the reaction temperature. Finally, the magnetic properties of representative samples have been studied at 5 K and room temperature.

P. Dallas · A. B. Bourlinos (✉) ·
D. Niarchos · D. Petridis
NCSR Demokritos, Institute of Materials Science,
Aghia Paraskevi Attikis, Athens 15310, Greece
e-mail: bourlinos@ims.demokritos.gr

Introduction

Magnetic nanoparticles have been the focus of intense research due to their size dependent properties [1] and their various applications, like in the information storage industry [2], as high-density recording media [3] and in several biomedical applications, such as in Magnetic Resonance Imaging (MRI) contrast agents [4], carriers in drug delivery experiments [5] and magnetic induced hyperthermia [6].

Organic surfactants modify the surface of the nanoparticles in order to provide them with solubility, to prevent their aggregation or to act as carriers of biologically active molecules [7]. Ferrofluids define a unique class of magnetic particles soluble in organic (organosols) [8], or aqueous (hydrosols) solvents [9]. Usually, organic moieties are bound to the surface either through covalent bonding between a functional group and the surface atoms (chemisorption) or weak Van Der Waals interactions (physisorption). Physisorbed molecules can form more than one layer on the nanoparticle surface, while chemisorbed molecules usually appear as a monolayer. In addition, layers of physisorbed capping agents can be built on top of the chemisorbed surfactants [10]. Typical surface modifiers include long chain alkyl amines, phosphines or carboxylic acids [11–14]. Furthermore, primarily used coatings can be replaced by other surfactants through an exchange ligand process [15]. Accordingly, surface functionalization is a key process towards reconstructed derivatives suitable for certain demands.

On the other hand, since the properties of nanoparticles are size and shape dependent, size control via manipulation of the reaction conditions is of prime interest [16]. For instance, high temperatures tend to

lead to the formation of more nucleus, and therefore, to smaller nanoparticles. In contrast, low temperatures favour the opposite effect. Lastly, aging of the reaction mixture leads to aggregates and the formation of larger particles [17]. As a result, both surface modification and size control affect the magnetic properties of the nanoparticles by reducing the dipole interactions, the surface and the total anisotropy [18].

In this work we study the synthesis of iron oxide nanoparticles through a water/toluene biphase system in presence of surfactants. The experimental details are expanding the synthesis proposed in a previously published procedure [19]. Emphasis is given to the size control of the nanoparticles through variation of both reaction conditions and surfactant, as well as, to the study of the coordination mode of the surfactants. Finally, the magnetic properties of the resulting nanoparticles were studied at 5 K and room temperature.

Experimental part

Synthesis of neat magnetic iron oxide nanoparticles

A 1.25 g $FeSO_4 \cdot 7H_2O$ and 0.6 g KOH was dissolved in 30 mL H_2O of prefixed temperature. Following, 0.5 mL of diluted H_2O_2 (2%) was added. The mixture was refluxed for 1 h. Two samples were prepared, sample A_1 (25 °C) and sample A_2 (50 °C), whereby the numbers in parentheses denote the temperature of the aqueous phase prior dissolution of the iron salt and KOH. The as-prepared magnetic solids were insoluble in aqueous or organic media. They were isolated by centrifugation, washing with water and drying.

Oleic acid magnetic derivatives

A 1.25 g $FeSO_4 \cdot 7H_2O$ and 0.6 g KOH was dissolved in 30 mL H_2O of prefixed temperature. Then, 0.5 mL of diluted H_2O_2 (2%) was added. Following, 30 mL of toluene containing dissolved 2.5 mL of oleic acid were added. The mixture was refluxed for 1 h, whereupon the magnetic nanoparticles were extracted to the organic layer. The biphase mixture was cooled at room temperature until the two phases were clearly separated. After separation of the deep brown organic phase the product was isolated by adding 40 mL acetone, centrifugation of the resultant precipitate and subsequent washing by the same solvent. Three samples were prepared as above: sample B_1 (25 °C), sample B_2 (50 °C) and sample B_3 (60 °C). The magnetic products are highly soluble in organic solvents such as toluene, chloroform and hexane. In a post-treatment, the uncoated iron oxide sample A_2 was surface treated with oleic acid in ethanol, followed by centrifugation, washing with acetone and drying.

Oleylamine magnetic derivatives

The particular derivatives were prepared similarly as above except using oleylamine in place of oleic acid. The samples are: C_1 (25 °C), C_2 (50 °C) and C_3 (60 °C). All magnetic solids are highly soluble in organic solvents as above.

Characterization of the products

X Ray Diffraction patterns were recorded on powder samples by a Siemens 500 Diffractometer with a scan rate of 0.015° per second. Transmission Electron Microscopy observations were carried out in a Jeol 100 CX electron microscope operating at 100 kV. Thermogravimetric measurements (TGA) were performed on a Perkin-Elmer Pyris TGA/DTA under airflow. Hysteresis curves were recorded in a Superconductive Quantum Interference Device (SQUID) in an external magnetic field from –5 to 5 T. Infrared (FT-IR) spectroscopy studies were performed on a Nicolet 20 SXC spectrometer using KBr pellets (Aldrich, 99%, FT-IR grade). The ^{57}Fe Mössbauer spectra were obtained at 4.2 K (LHe), 77 K (LN) and 300 K (RT) on a conventional constant acceleration spectrometer with a ^{57}Co(Rh) source moving at RT.

Results and discussion

Magnetic nanoparticles were prepared in different sizes by changing the temperature of the aqueous phase at the beginning of the reaction. The presence of surfactants as capping agents additionally affects the size of the particles. Figure 1 shows the XRD patterns and the corresponding crystal plains of all as-synthesized iron oxide samples. By applying the Scherrer equation to the most intense peak, i.e. (311), we obtained the average size of the magnetic nanoparticles. These results are summarized in Table 1.

As a general trend, increment of the temperature of the aqueous phase prior addition of the reagents leads to the formation of nanoparticles with reduced mean diameter. Furthermore, functionalization of the surface by surfactants intervenes in the crystal growth process inducing a further decrease in the nanoclusters' crystal

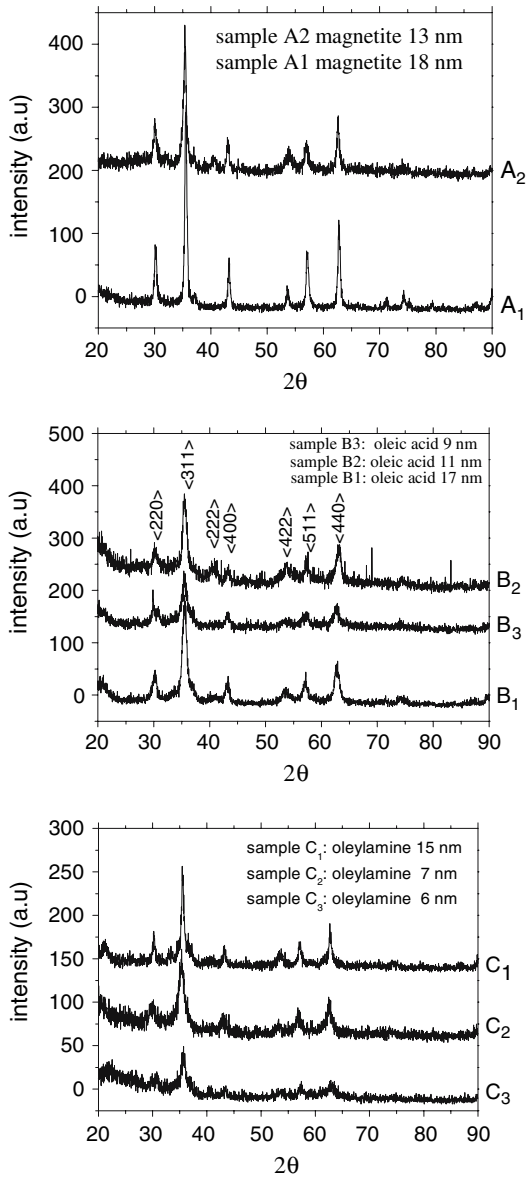

Fig. 1 XRD patterns for the: (**a**) iron oxide samples A_1, A_2; (**b**) iron oxide samples B_1, B_2 and B_3 coated with oleic acid; (**c**) iron oxide samples C_1, C_2, C_3 coated with oleylamine

Table 1 The size of the magnetic nanoparticles at different experimental conditions. (* Temperature at the beginning of the reaction)

Sample/surfactant	Mean Size (nm)	Temperature* (°C)
A_1, A_2	18, 13	25, 50
B_1, B_2, B_3/oleic acid	17, 11, 9	25, 50, 60
C_1, C_2, C_3/oleyl amine	15, 7, 6	25, 50, 60

size. The comparison between the oleic acid and oleylamine capped iron oxide nanoparticles under similar reaction conditions reveals that surface modification with oleylamine further blocks the crystal growth, thus leading to the formation of smaller nanoparticles. In order to identify the effect of the surface functionalization to the reduced crystal growth, a control experiment was performed in absence of surfactants. In this case, the synthesis of neat magnetic iron oxide nanoparticles (without addition of toluene and surfactants) was performed at two different temperatures keeping constant concentrations. At both initial temperatures, 25 °C and 50 °C, the mean size of the resulting nanoparticles was higher than that of the oleic acid and oleylamine mediated procedures meaning that the capping agents stop the crystal growth of the iron oxide nanoparticles.

As maghemite and magnetite are isostructural, the XRD technique cannot clearly differentiate between them, especially in the nanophase state where the characteristic reflections are broad and appear almost at the same 2θ positions. Mössbauer spectroscopy can clearly identify between the two magnetic iron oxides due to the presence of divalent iron in magnetite. The spectrum recorded at 5 K for B_1 sample, bottom in Fig. 2, left, was fitted with two sextets (A and B) with the following parameters: site A I.S (isomer shift) = 0.32 mm/s, Q.S (quadropole splitting) = 0, H_h (hyperfine field) = 489 Oe. Site B I.S = 0.58 mm/s, Q.S = 0, H_h = 450 Oe. The high I.S value for site B, which lies between those of trivalent and divalent iron, indicates the presence of Fe (II) and accordingly formation of Fe_3O_4. Similarly, the values of H_h are consistent with the magnetite phase [20]. Moreover, the Mössbauer spectra recorded at different temperatures, Fig. 2(a–c), are indicative of small particles exhibiting superparamagnetism, meaning that a fine particle is able to reverse its magnetic moment by thermal activation in the timescale of the Moessbauer effect. More specifically, when the spectrum was recorded at room temperature a doublet appears, indicating superparamagnetism. At lower temperatures the spectrum exhibits the typical sextet of ferromagnetism. In superparamagnetic materials all spins of iron atoms within a particle point in the same direction, but thermal fluctuations cause this direction to vary with a frequency that depends upon the particle size, anisotropy energy and temperature. If this frequency is greater than the Larmor procession frequency of the ^{57}Fe nucleus (10^{-8} s^{-1}), the magnetic hyperfine splitting collapse to a singlet or doublet line, the later if a quadrapole interaction is present. In the opposite case of slow relaxation of the iron spins, a complete magnetic hyperfine splitting is observed. However, because of size distribution in a sample, the spectra consist of a doublet from small particles with short relaxation time, together with a sextet due to larger particles with

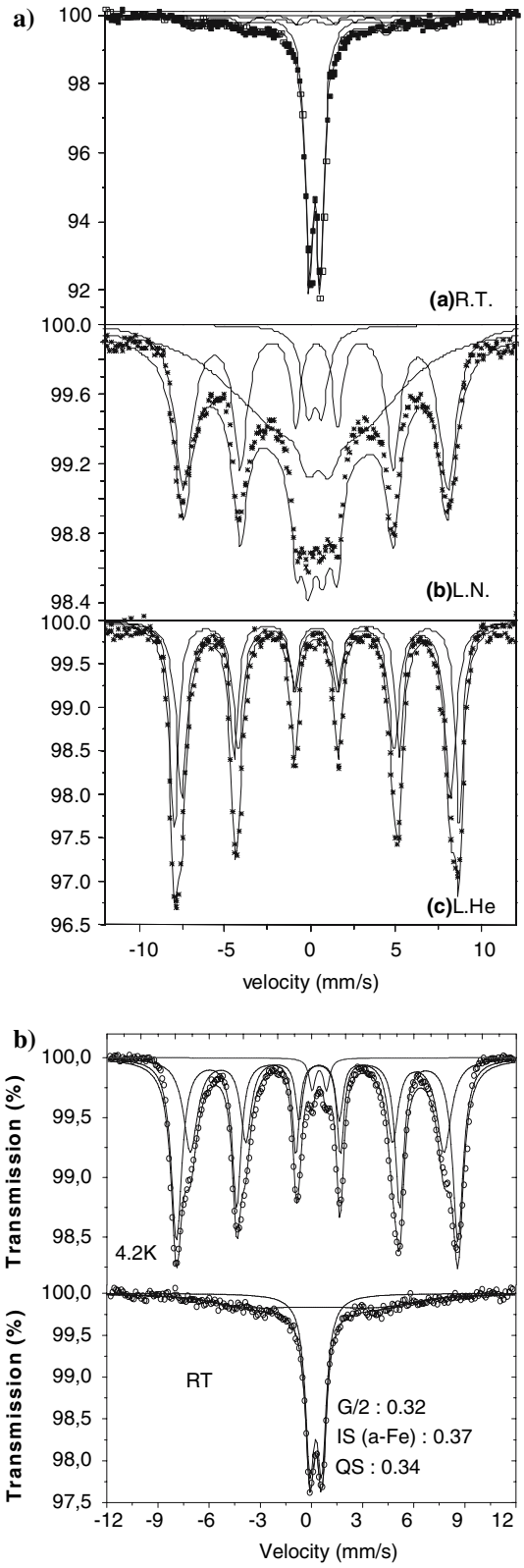

Fig. 2 Variable temperature Mössbauer spectra for two representative samples: (**a**) sample B_1, recorded at 300, 77 and 4.2 K (left); (**b**) sample B_3 recorded at 300 and 4.2 K

longer relaxation time [20]. Furthermore, the relative area of the doublet increases with increasing temperature as a result of increasing the relaxation frequency, while the magnetic sextet increases with lowering the temperature as the relaxation frequency slows down. According to this description, the variable temperature Mössbauer spectra demonstrate that the present magnetite particles capped with oleic acid are nanoscale objects with a distribution of sizes.

When the nanoparticles were prepared using a hot injection process (sample B_3) the Moessbauer response of the magnetic oxide establishes the presence of non-stoichiometric maghemite. The spectrum recorded at 4.2 K, top in Fig. 2d, was fitted with two sextets (A and B) with the following parameters: site A I.S (isomer shift) = 0.46 mm/s, Q.S (quadropole splitting) = 0, H_h (hyperfine field) = 514 Oe. Site B I.S = 0.49 mm/s, Q.S = 0, H_h = 464 Oe. The I.S values are assigned to trivalent iron, indicating the formation of γ-Fe_2O_3, i.e. maghemite. In line with this observation, the RT spectrum shows a doublet with IS (0.37 mm/s) and QS (0.34 mm/s) parameters which are typical for the trivalent iron. Therefore, Mössbauer study of samples B_1 and B_3 demonstrates that low temperatures favour the formation of magnetite, while, higher initial temperatures lead to complete oxidation of divalent iron to trivalent and consequent formation of maghemite.

TEM images (Fig. 3) of products B_1 and B_3 show particles of cubic shape. Bright-field measurements performed on the 1–7 rings of the electron diffraction pattern of the B_1 sample, resulted in the following interatomic distances: $d_1 = 4.83$ nm, $d_2 = 2.95$ nm, $d_3 = 2.52$ nm, $d_4 = 2.08$ nm, $d_5 = 1.70$ nm, $d_6 = 1.61$ nm and $d_7 = 1.48$ nm. These values match the interplanar spacings of the crystal planes of magnetite (Fe_3O_4).

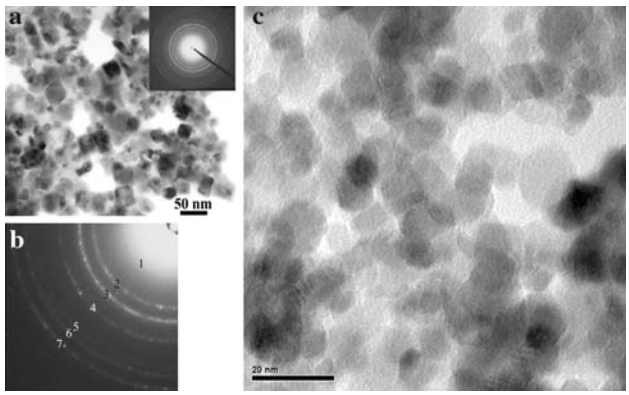

Fig. 3 (**a**, **b**) TEM micrographs and electron diffraction pattern for sample B_1; (**c**) TEM micrograph for sample B_3

The average diameter obtained from the TEM micrographs matches well the value calculated from the XRD patterns. The size distribution diagrams for sample B_3 is presented in Fig. 4.

The FT-IR spectrum reveals the nature of the bond that is formed between the surfactant and the surface atoms. In case of the oleic acid derivatives, the antisymmetric and symmetric vibrations at 2921 and 2850 cm^{-1}, respectively, are clearly observed due to the aliphatic alkyl chains (Fig. 5a). The presence of two peaks at 1517 and 1420 cm^{-1}, attributed to the carboxylate unit vibration modes, shows that oleic acid is bound through the carboxylate anions, i.e. chemisorption of the surfactant on the iron oxide surface. Except the chemisorbed amount, a physisorbed part was also present as evidenced by a less intense peak at 1721 cm^{-1} (-COOH). The FT-IR of the oleylamine analogues also shows the intense adsorption peaks at 2921 and 2850 cm^{-1} attributed to the alkyl chains. The bands attributed to the antisymmetric and symmetric vibration modes of -N-H are observed at 3438 and 3224 cm^{-1} respectively (Fig. 5b). Due to the coordination of the unpaired electron couple of the nitrogen atom, the vibration bands are observed in lower values than those expected for the free amine group, i.e. 3500 and 3300 cm^{-1} respectively. This indicates that oleylamine is bound on the surface through the unpaired electron couple of the amine group.

When the magnetite sample A_2 was post-treated with oleic acid in ethanol, the corresponding FT-IR spectrum (Fig. 5c) exhibited a rather intense peak at 1716 cm^{-1} showing a physisorption process. The vibration modes of the carboxylate anion were also observed but with a weaker intensity. Therefore it seems that the in situ synthesis of coated magnetite nanoparticles under biphase conditions leads to chemisorption. On the other hand, post-treatment with oleic acid favours a physisorption process.

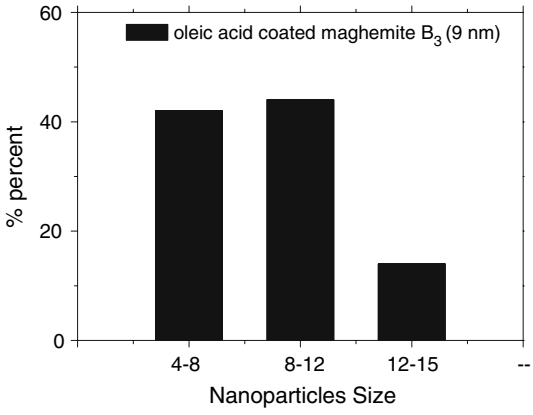

Fig. 4 Characteristic size distribution diagrams for sample B_3

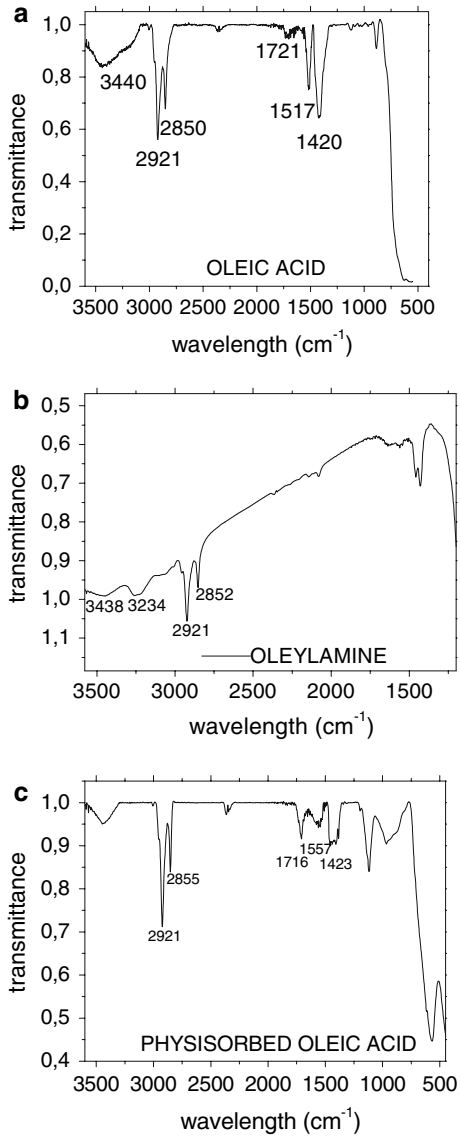

Fig. 5 FT-IR spectra of magnetic iron oxides coated with: (**a**) oleic acid; synthesized from a biphase system. (**b**) oleylamine; synthesized through a biphase system. (**c**) oleic acid from mixing oleic acid and neat iron oxide nanoparticles in ethanol

The coordination mode of the chemisorbed capping agents to the metal sites on the surface of the nanoparticles was also identified by FT-IR spectroscopy. According to previous references the difference between symmetric and asymmetric vibration depends on the coordination mode [21]. In oleic acid the difference is 97 cm^{-1}, clearly showing a chelating bidentate coordination mode. In the case of the post-treated sample, the relatively small amount of chemisorbed oleic acid exhibits a difference of ~134 cm^{-1} that is assigned to the bridging bidentate coordination.

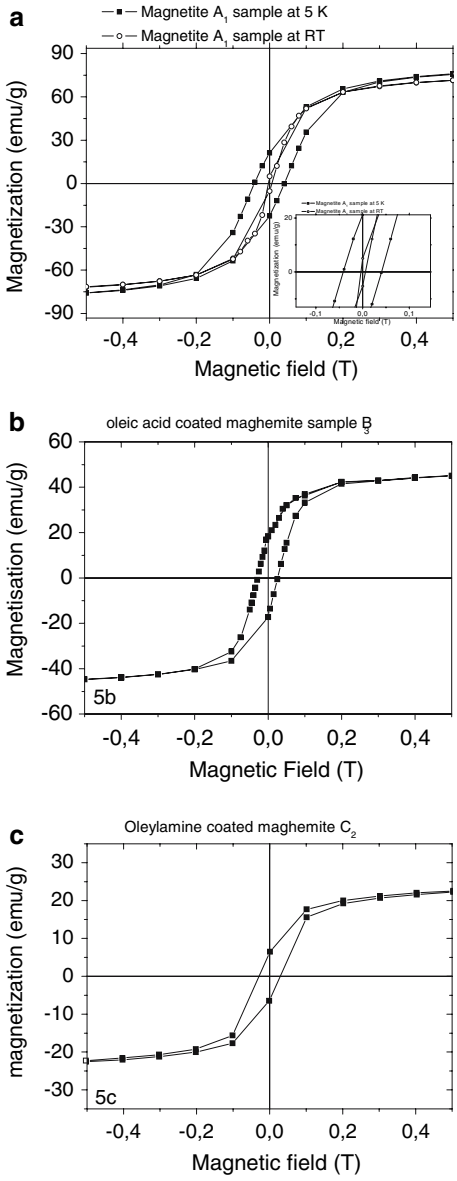

Fig. 6 Magnetization curves of: (**a**) sample A_1 with no surfactants recorded at 5 K and RT (**b**) capped with oleic acid nanoparticles recorded at 5 K (sample B_3); (**c**) capped with oleylamine nanoparticles recorded at 5 K (C_2 sample)

The next step was the study of the magnetic properties. At room temperature, iron oxide nanoparticles do not exhibit hysteresis, with almost zero coercivity. However, at 5 K thermal fluctuations become negligible and therefore the material exhibits significantly higher coercivity values as it is clearly indicated from the magnetization curves (Fig. 6). The magnetization curves for the sample A_1 recorded at RT and 5 K are presented in Fig. 6a. At room temperature there is a significantly low coercivity, its value is about 40 Oe and can be considered as negligible. In contrast the freezing of the spins at low temperatures give rise to a coercive field value of about 400 Oe at 5 K. Accordingly the remanesence magnetization follows a similar increase from a significant low value at RT (about 5 emu g^{-1}) to 21 emu g^{-1} at 5 K. A slight increase of the saturation magnetization is also observed from RT to 5 K.

Table 2 Magnetic properties for maghemite capped with different surfactants. The measurements were performed at 5 K

Sample	Size	Magnetization (emu/g)	Coercivity (Oe)
A_1 (at RT)	18 nm	75	40
A_1 (at 5 K)	18 nm	80	410
B_3	9 nm	60	282
C_2	7 nm	40	285

In Table 2 the saturation magnetization and the coercivity of the representative iron oxide nanoparticles are presented. The magnetization is calculated taking into consideration the amount of the capping agents, based on TGA, so the values correspond to pure iron oxide. A representative thermograph for the oleic acid capped iron oxide (sample B_3) can be seen in Fig. 7. The weight percentage of the organic surfactants is about 24% of the total weight. Actually, the high percentage of the organic part contributes to the high solubility of the nanoparticles in common organic solvents such as toluene and chloroform and in turn to the colloidal stability of the dispersions.

Both samples, oleic acid and oleylamine capped maghemite nanoparticles, exhibit the same coercivity values. However the magnetization of the oleic acid capped maghemite is higher than that of the oleylamine analogue due to its larger mean diameter. Overall, the magnetization data are both in a good agreement with those previously reported for nanosized maghemite nanoparticles [22].

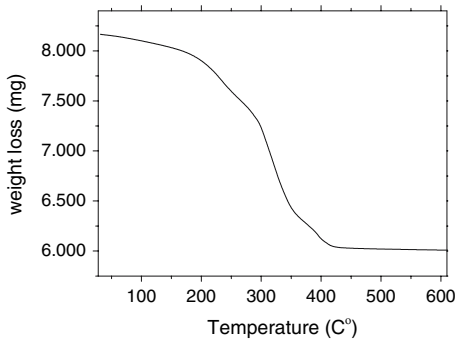

Fig. 7 TGA trace for the oleic acid coated iron oxide nanoparticles (sample B_3) indicating the % wt of the organic surfactants

Conclusions

In this work we report results on the synthesis of iron oxide nanoparticles through a biphase system, on the surface coating and coordination mode of various surfactant molecules on the surface of the synthesized Fe_3O_4 or γ-Fe_2O_3 nanoparticles. Highly soluble and stable for several months organosols have been synthesized. The effect of the reaction temperature and the type of surfactant upon the mean size and magnetic properties of the nanoparticles are presented. We conclude that high temperatures during the addition of the reagents favour a lower mean size for the nanoparticles and the formation of maghemite. Additionally, functionalization with capping agents further blocks crystal growth thus reducing the nanoparticles' dimensions. Magnetization curves and Mössbauer spectroscopy measurements indicate the magnetic nature of the nanoparticles showing a superparamagnetic behaviour at room temperature.

References

1. Kodama RH (1999) J Magn Magn Mat 200:359
2. Sun S, Murray CB, Weller D, Folks L, Moser A (2000) Science 287:1989
3. Dai ZR, Sun S, Wang ZL (2001) Nano Lett 1:443
4. a) Martin CR, Mitchell DT (1998) Anal Chem 70:322; (b) Portet D, Denizot B, Rump E, Lejeune J, Jallot P (2001) J Colloid Interface Sci 238:37
5. Viroonchatapan E, Sato H, Ueno M, Adachi I, Tazawa K, Horikoshi I, (1997) J Control Release 46:263
6. Jordan A, Schol R, Maier KH, Johannsen M, Wust P, Nadobny J, Schirra H, Schmidt H, Deger S, Loening S, Lanksch W, Felix R (2001) J Magn Magn Mat 225:118
7. McIntosh CM, Esposito EA, Boal AK, Simard J, Martin CT, Rotello VM (2001) J Am Chem Soc 123:7626
8. Bourlinos AB, Simopoulos A, Petridis D (2002) Chem Mater 14:899
9. Yokoi H, Kantoh T, (1993) Bull Chem Soc Jpn 66:1536
10. Selwood PW (1975) Chemisorption and magnetization. Academic Press, New York
11. Boal A, Das K, Gray M, Rotelo V (2002) Chem Mater 14:2628
12. a) Buckland CH, Rochester SA, Topman A (1980) J Chem Soc Faraday Trans 1:302; (b) Rochester CH, Topman SA (1979) J Chem Soc Faraday Trans 1:872
13. a) Brust M, Walker M, Bethel D, Schiffrin DJ, Whyman R (1994) Chem Commun 801; (b) Mayer MM, Luo J, Lin Y, Egelhart MH, Hepel M, Zhong CJ, (2003) Langmuir 19:25
14. Green M, O'Brien P (1999) Chem Commun 2235
15. Son SU, Jang Y, Yoon KY, Kang E, Hyeon T (2004) Nano Lett 4:1147
16. Puntes VF, Krishman KM, Alivisatos AP (2001) Science 291:2115
17. Hyaeon T (2003) Chem Commun 927
18. Vestal CR, Zhang ZJ (2003) J Am Chem Soc 125:9828
19. Bourlinos AB, Bakandritsos A, Georgakilas V, Tzitzios V, Petridis D (2006) J Mater Sci 41:5250
20. Morup S, Damestic JA, Topsol H In: Cohen RL (ed) Applications of Moessbauer Spectroscopy, vol II. Academic Press, New York
21. Rocchicciolideltcheff C, Franck R, Cabuil V, Massart R (1987) J Chem Res Synop 5:126
22. a) Butterworth MD, Bell SA, Armes SP, Simpson AW (1996) J Colloid Interface Sci 183:91; (b) Chang HSW, Chiou CC, Chen YW (1997) J Solid State Chem 128:87